GEOPHYSICAL RESEARCH LETTERS, VOL. 36, L03815, doi:10.1029/2008GL036728, 2009

Click Here for Full Article

How often does it rain over the global oceans? The perspective from CloudSat

Todd D. Ellis,[1] Tristan L'Ecuyer,[2] John M. Haynes,[2] and Graeme L. Stephens[2]

Received 19 November 2008; accepted 6 January 2009; published 10 February 2009.

[1] The frequency of precipitation occurrence over the global oceans from 2006–2007 as calculated from CloudSat radar data is compared to ship-based (ICOADS) and island-based (GSOD) data. It is shown that the spatial pattern of the precipitation frequency from CloudSat is consistent with previous climatological studies. The comparison to ship-based data reveal that CloudSat results are consistent with ship observations well into the high latitudes and appear to capture the seasonal cycle of precipitation well. A comparison to island data also shows good qualitative agreement, although the spatial scale mismatch complicates the efficacy of such comparisons. Nevertheless, CloudSat is shown to be a viable platform for obtaining quality satellite-based precipitation frequency measurements. **Citation:** Ellis, T. D., T. L'Ecuyer, J. M. Haynes, and G. L. Stephens (2009), How often does it rain over the global oceans? The perspective from CloudSat, *Geophys. Res. Lett.*, *36*, L03815, doi:10.1029/2008GL036728.

1. Introduction

[2] Observing changes in global precipitation is a topic of vital importance to the scientific community. Several recent studies [e.g., *Allen and Ingram*, 2002; *Held and Soden*, 2000; *Stephens and Ellis*, 2008] have argued that there are robust physical reasons why this total precipitation must decrease in response to an increase in carbon dioxide in the atmosphere. *Trenberth et al.* [2003] argue that the nature of these changes are such that the character of precipitation should change, with events becoming less frequent and more intense. Interestingly, it has been shown that while climate models may predict future decreases in global precipitation frequency, they often do so through an incorrect combination of frequency and intensity [*Sun et al.*, 2006, and references therein]. To increase scientific confidence in such predictions, climate models should be able to reproduce the frequency and intensity of precipitation as observed in the current climate system.

[3] The problem, therefore, is selecting and vetting the data to be used for verification of the satellite observations. Ground based data [i.e., *Sun et al.*, 2006; *Dai*, 2001] and ship-based data [i.e., *Petty*, 1995] have been used repeatedly for such purposes. However, technical challenges arise because such data are not global or homogeneous and are often taken by various observing platforms. Conventional satellite-based observations of precipitation frequency on the other hand, provide global coverage but suffer from a lack of sensitivity to light precipitation either due to instrument limitations or an inability to distinguish between light rain and cloud [*Berg et al.*, 2006]. *Petty* [1997] found that ten special sensor microwave/imager retrieval algorithms often failed to detect precipitation at high latitudes or in regions of showery trade cumulus precipitation. Given that *Haynes and Stephens* [2007] showed that trade cumulus precipitation likely occurs more frequently than originally believed, this is a serious shortcoming.

[4] The twofold goals of this report are: (1) to evaluate the use of a millimeter-wave radar system (the Cloud Profiling Radar (CPR) [*Im et al.*, 2005]) on board the CloudSat satellite flying as part of the A-Train satellite constellation [*Stephens et al.*, 2002] to detect precipitation over the global oceans, and (2) to then use CloudSat to characterize the global distribution of precipitation incidence during its two years in orbit.

2. Data and Methods

[5] The combination of path-integrated attenuation (PIA) and high sensitivity radar reflectivity observations from CloudSat's 94 GHz (W-band) nadir-pointing CPR provide the ideal combination of measurements for detecting precipitation with a high degree of confidence. *Haynes et al.* [2009], for example, outline an approach that uses surface wind speed, sea surface temperature, and atmospheric temperature and moisture profiles over the oceans from the European Centre for Medium-range Weather Forecasting (ECMWF) weather model to determine the theoretical backscatter cross section of the surface in the absence of hydrometeors. Comparison of the radar-observed backscatter cross section against this theoretical model provides a means of measuring the PIA, which in turn can be used to detect the presence, and often the intensity, of precipitation.

[6] Following *Haynes et al.* [2009] the sum of the observed near-surface radar reflectivity (480 m and 720 m above sea level) and the contributions from PIA and gaseous attenuation provides an estimate of the unattenuated near-surface reflectivity value. The larger the value, the more likely that precipitation is occurring. Thus, threshold values of this reflectivity can be chosen to indicate the likelihood of precipitation. For rain, the threshold reflectivity over which precipitation is certainly occurring is approximately 0 dB [*Schumacher and Houze*, 2000]; reflectivities between −15 dB and 0 dB indicate that drizzle is probably occurring [*Frisch et al.*, 1995, *Stevens et al.*, 2003]. For snow (i.e., when the entire atmospheric temperature profile is below 0°C), the threshold for certain precipitation is approximately −5 dB. The result is an algorithm that,

[1]Department of Earth Sciences, State University of New York College at Oneonta, Oneonta, New York, USA.

[2]Department of Atmospheric Science, Colorado State University, Fort Collins, Colorado, USA.

0094-8276/09/2008GL036728$05.00

Table 1. WMO Present Weather Codes Used to Classify Precipitation Events as Possibly or Certainly Detectable by CloudSat[a]

Certain	Possible
50, 51, 52, 53, 54, 55, 58, 59, 60, 61, 62, 63, 64, 65, 80, 81, 82, 91, 92	13, 14, 15, 16, 17, 18, 19, 20, 21, 23, 24, 25, 26, 27, 29, 56, 57, 66, 67, 68, 69, 83, 84, 87, 88, 89, 90, 93, 94, 95, 96, 97, 98, 99

[a]See *Dai* [2001, Table 1] for a description of these codes.

unlike other spaceborne precipitation radars, is sufficiently sensitive to the presence of small water droplets that even incipient precipitation can be detected [*Stephens and Haynes*, 2007]. Furthermore, unlike passive microwave sensors that suffer from an inability to distinguish cloud and precipitating liquid, the use of reflectivity ensures that sufficient numbers of large droplets exist to guarantee the presence of precipitation. In heavy rain events when the CPR signal may be fully attenuated, this algorithm will still mark the presence of precipitation, allowing the detection of precipitation events across a full spectrum of intensities.

[7] To evaluate this product, it is compared with two existing data sets that provide precipitation occurrence data over the oceans, albeit with much less spatial coverage: the International Comprehensive Ocean-Atmosphere Data Set (ICOADS) 2.4 ship-based data [*Worley et al.*, 2005], and Global Summary of the Day (GSOD) precipitation data [*Lott and Baldwin*, 2002] available from the National Climatic Data Center (NCDC). The ICOADS dataset includes standard ship synoptic weather data as well as a series of valuable quality control flags that can be used to parse those data. This study constructs a global-ocean climatology of frequency of precipitation occurrence using the present weather (WMO code "ww") and cloud amount (WMO code "N") reports extracted from the ICOADS dataset for the time period covering August 2006–July 2007.

[8] In this study, we closely approximate the methods of *Dai* [2001] and *Petty* [1995], including the extensive quality control measures used to avoid various human observing errors. The main difference from those studies comes from our selection of a different subset of the present weather codes as defined in Table 1, including rain and snow, so to represent both "possible" and "certain" precipitation events that CloudSat might be able to detect. While "certain" events are those that would definitely be detected by the CPR, "possible" events include a variety of reports including: precipitation reported within sight of, but not at the ship, events related to precipitation (such as lightning) but without an actual precipitation report, precipitation in the hour preceding the observation, potentially small-scale events such as thunderstorms and showers, and freezing rain. Due to limited space, we must refer the reader to the extensive listing of *Dai* [2001, Table 1] for more details on these classifications. Any code omitted from Table 1 is classified as non-precipitating. More importantly, the difference between the number of observations that include only "certain" precipitation events and the number of observations that include both "possible" and "certain" precipitation provides a range of acceptable values of frequency of precipitation occurrence for comparison to the satellite observations. Finally, due to the spatial inhomogeneity of ship-based reports, both the ICOADS reports and CloudSat data are zonally averaged into 2.5 degree latitude bands. This also has the advantages of increasing the number of observations used in the calculation and giving us a more global sense of the agreement between CloudSat and the ship-based observations.

[9] However, one drawback of performing zonal averages is that they eliminate the opportunity to evaluate precipitation occurrence statistics for individual locations and/or individual systems. To address this concern, we have also chosen to compare daily precipitation reports extracted from the GSOD dataset for nine islands from disparate locations listed in Table 2. In selecting these locations, care was taken to select island locales that were low in elevation so to obtain climates that would be less like land-based stations and more like ocean sites. These data, which span the years 1929 through present, report eighteen surface meteorological elements for each day (0000–2359 UTC) and represent ranges and averages from synoptic and hourly data sources. These observations are run through extensive automated quality control to be considered valid and at least four separate valid observations per day are required to create one valid daily datum.

[10] For this study, GSOD data from August 2006–July 2007 are used to coincide with the other two datasets. However, since GSOD data only provide total daily precipitation, we can only compare "rain days," which we define as a day when non-zero liquid equivalent precipitation or a trace of precipitation (precipitation flag "H") was reported in the GSOD data or a day when CloudSat measured a non-zero rain rate in the box around the station. We must also note the difficulty in comparing a surface observation at a point to a satellite observation that may not pass directly overhead. To address this, we include any CloudSat observations that pass within the 2.5 × 2.5 degree box centered on the station's location on a given day. While this may artificially inflate the number of "rain days" CloudSat detects, using a smaller bounding box results in too few observations to obtain a reliable estimate of precipitation occurrence.

3. Results and Discussion

[11] Figure 1 presents zonal-mean comparisons of the CloudSat frequency of precipitation occurrence, including certain rain events (asterisks), certain rain and certain snow

Table 2. Selected GSOD Island Stations and the Number of Observations Used to Calculate Frequencies of Precipitation Occurrence Shown in Figure 2

Index	Location	Latitude	Longitude	# Obs. (GSOD)	# Obs. (CloudSat)
A	Stornoway, UK	58.2° N	6.3° W	365	116
B	Male, Maldives	4.2° N	73.5° E	365	85
C	Naha, Okinawa, JP	26.2 °N	127.7° E	365	85
D	Ascension Is.	8.0° S	14.4° W	365	65
E	Mauritius	16.5 °S	59.6° E	365	88
F	Adak, AK, USA	51.9 °S	176.7° W	365	86
G	Guam Is., USA	13.5 °N	143.2° E	365	45
H	Tarawa Is., USA	1.35 °N	172.9° E	365	86
I	Invercargill, NZ	46.4 °S	168.3° E	365	86

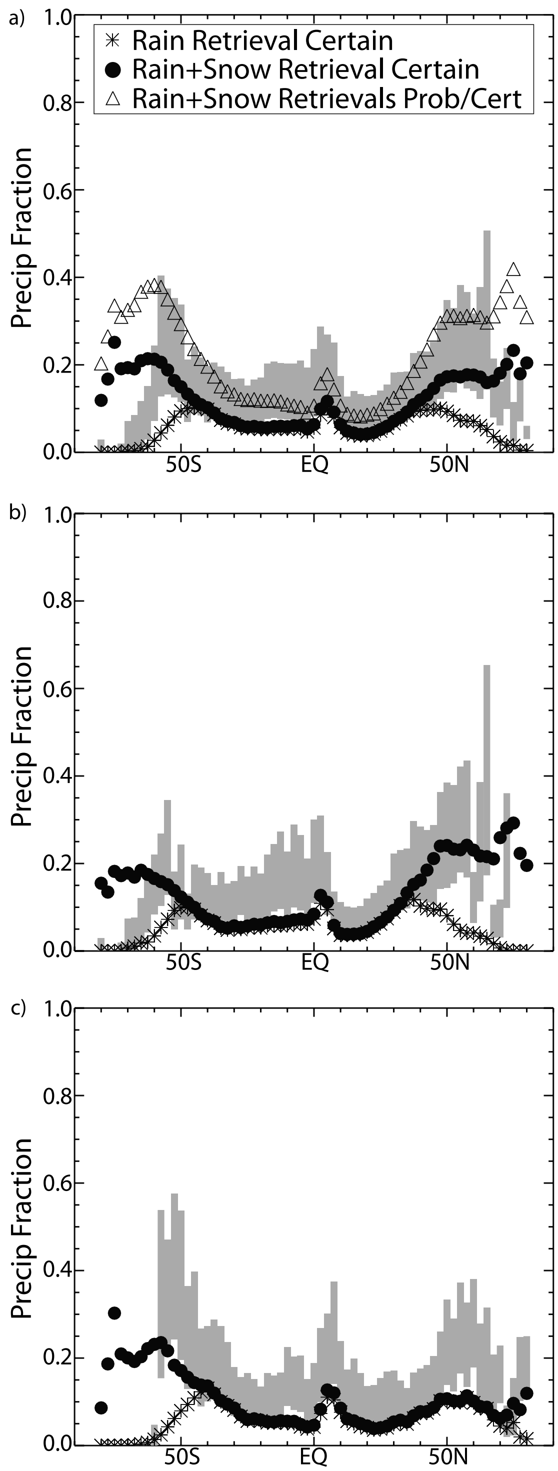

Figure 1. Zonal-mean comparison of precipitation frequency in 2006–2007 as retrieved by CloudSat. Stars represent certain rain retrievals, circles represent certain rain or snow retrievals, and triangles represent somewhat more uncertain rain or snow events. These are plotted against the range of possible frequencies derived from ship-based weather reports from the ICOADS dataset (grey bars). (a) Depictions of annual mean, (b) boreal summer (JJA), and (c) austral summer (DJF).

events (filled circles), and rain and snow events that are classified as either probable or certain (triangles) to the ICOADS ship-based reports (grey bars) in the annual mean (Figure 1a), in boreal summer (Figure 1b), and in austral summer (Figure 1c). The meridional patterns of precipitation exhibited in these plots are consistent with the results of *Petty* [1995], both seasonally and in the annual mean, given that the ITCZ is evident in all plots, as well as increased precipitation due to winter hemisphere mid-latitude storms.

[12] There are several other main points that we wish to call to the reader's attention:

[13] (i) In the annual mean (Figure 1a), the frequency of occurrence of rain and snow when the CloudSat retrieval is certain largely falls within the range of values one would expect based on the ICOADS data between the latitudes of 60°S and 70°N;

[14] (ii) The retrieval of snow appears, based on analysis of Figures 1a–1c, to perform very well, as evidenced by the difference between the rain only and combined rain/snow data in the winter hemispheres and because the combined rain/snow data fall within the range provided by ICOADS;

[15] (iii) The seasonal cycle of precipitation frequency, as illustrated in Figures 1b and 1c, detected by CloudSat is also consistent with that observed from the ICOADS data;

[16] (iv) It is impossible to evaluate the performance of CloudSat poleward of 60°S or 70°N due to a lack of ship-based data. In these regions, there are fewer than 10 ship observations for the entire year.

[17] (v) The CloudSat observations are at the low end of the ICOADS range of precipitation frequency observations, and in some cases (particularly in the tropics) the CloudSat data appear to indicate fewer instances of precipitation than ICOADS. We submit that this is due to the strict constraints that we have placed on this comparison. For the sake of comparison, we included CloudSat observations flagged as probable rain or snow events in Figure 1a, the CloudSat data falls well within the ICOADS ranges. In general, we feel that it is more instructive to show that, even using the most strict thresholds, the performance of the CloudSat retrieval is consistent with the ship-based data.

[18] Figure 2 shows how the CloudSat data compare to the selected GSOD stations (Table 2) for the period from August 2006–July 2007. Overall, the number of rain days as determined from CloudSat compares favorably to those determined from the station data from GSOD. In seven out of nine cases, CloudSat was within 15% of the GSOD data. We submit that this is quite good agreement considering that we are comparing satellite observations in a 2.5 $\times$ 2.5 degree box around the station to a point observation. In seven of the nine cases, CloudSat detected more rain days than the station reported. As mentioned in the previous section, this may be expected since, by including a larger possible area, the probability of precipitation occurring within that area would necessarily increase. Yet, some of the larger discrepancies are difficult to explain. At point D, Ascension Island, the 45% gap in rain days may be due to natural phenomena, it may be due to the larger area observed by CloudSat, it may be due to some bias in the ground based observations, or some combination of the three. Certainly further study on a case by case basis is warranted in order to understand the nuances of this analysis. Yet, the larger point that CloudSat can retrieve

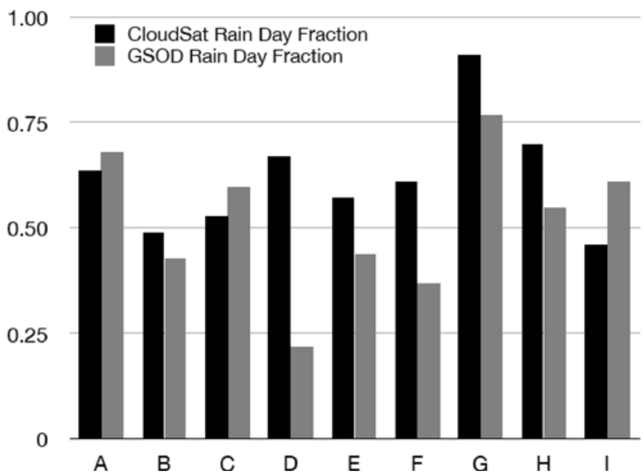

Figure 2. Comparison of number of rain days in 2006–2007 calculated at nine selected island stations (see Table 2 for locations) versus the number of rain days observed by CloudSat in the 2.5 × 2.5 degree box centered on that station.

precipitation frequencies that resemble those calculated from ground observations remains valid despite these uncertainties.

[19] Given the favorable comparisons with ICOADS and GSOD, we conclude by examining the global distribution of precipitation incidence from the first two years of CloudSat observations. Figure 3a presents a 2.5 × 2.5 degree map of the annual mean of the precipitation frequency including scenes classified as certain rain and certain snow spanning the period from August 2006 through July 2007. Notable features in Figure 3a include the relatively high frequencies of precipitation occurrence (greater than 20%) in the inter-tropical convergence zone (ITCZ) and the mid-latitude storm tracks roughly poleward of 40 degrees latitude. Though not shown, much of the precipitation observed by CloudSat poleward of 50 degrees latitude is classified as snow. The global mean precipitation incidence derived from this map is 10.9%; the global mean including only rain is 8.7%. Figure 3b shows the zonal-mean seasonal cycle of precipitation (rain and snow) as observed by CloudSat. Particularly notable are: (i) the reduced precipitation in the midlatitudes in both hemispheres in summer due to reduced baroclinicity in the summer months; (ii) the northward shift of the tropical precipitation in the boreal summer and fall due to the seasonal migration of the ITCZ, and (iii) the larger amplitude of the seasonal cycle in the northern hemisphere, which is likely due to the larger baroclinicity due to the greater land mass. These observations, particularly those regarding precipitation in the poleward of the tropics, showcase the utility of the observations that CloudSat is uniquely situated to provide.

4. Concluding Remarks

[20] CloudSat radar observations of the frequency of precipitation incidence over the oceans for a period spanning August 2006–July 2007 compare favorably to concurrent ship based and island based station observations and show a number of interesting features about the global distribution of the incidence of rain and snow. Specifically, the results of this study reveal a number of promising findings:

[21] (i) The most conservative measures of both the annual mean and the seasonal cycle of the zonal-mean frequency of precipitation occurrence from CloudSat fall within a range of values from the ICOADS dataset that are believed to represent precipitation events that may be detectable from space;

[22] (ii) CloudSat observations of precipitation are in agreement with ship based observations well into the high latitudes, providing a unique satellite-based observation of these precipitation events for the first time;

[23] (iii) A comparison of the number of rainy days as calculated from island station data to the number of rainy days as calculated in a 2.5 × 2.5 degree box around the station from CloudSat observations show remarkable agreement despite the apparent difficulties of comparing point data to an entire grid square average;

[24] (iv) Most importantly, CloudSat observations of precipitation incidence demonstrate a near global distribution of precipitation frequency, the high incidence of rain and snow in the midlatitudes, and the seasonality of

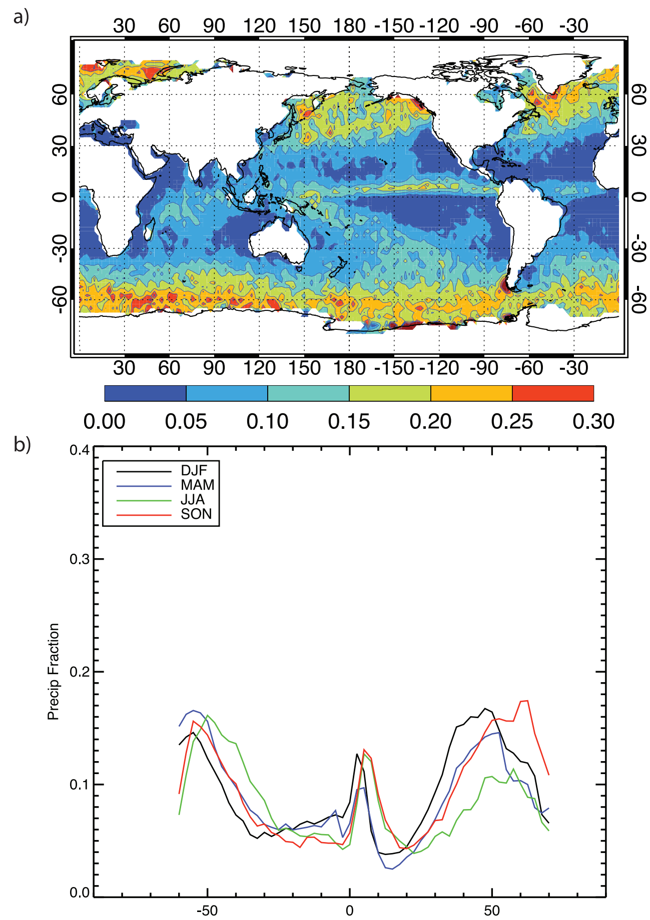

Figure 3. The frequency of precipitation incidence as observed by CloudSat. (a) Map of global distribution including both rain and snow. (b) Zonal-mean seasonal cycle of precipitation incidence.

precipitation in the midlatitudes, particularly in the northern hemisphere.

[25] **Acknowledgments.** We wish to extend great thanks to Steve Worley, Scott Woodruff, Zaihua Ji and any others associated with the ICOADS project who rushed to make June and July 2007 data available to us for this study. This study was funded by NASA CloudSat research grant NNX07AR97G.

References

Allen, M. A., and W. J. Ingram (2002), Constraints on future changes in climate and the hydrologic cycle, *Nature*, *419*, 224–232, doi:10.1038/nature01092.

Berg, W., T. L'Ecuyer, and C. Kummerow (2006), Rainfall climate regimes: The relationship of regional TRMM rainfall biases to the environment, *J. Appl. Meteorol. Climatol.*, *45*, 434–454, doi:10.1175/JAM2331.1.

Dai, A. (2001), Global precipitation and thunderstorm frequencies. Part I: Seasonal and interannual variations, *J. Clim.*, *14*, 1092–1111, doi:10.1175/1520-0442(2001)014<1092:GPATFP>2.0.CO;2.

Frisch, A. S., C. W. Fairall, and J. B. Snider (1995), Measurement of stratus cloud and drizzle parameters in ASTEX with a K_α-band Doppler radar and a microwave radiometer, *J. Atmos. Sci.*, *52*, 2788–2799, doi:10.1175/1520-0469(1995)052<2788:MOSCAD>2.0.CO;2.

Haynes, J. M., and G. L. Stephens (2007), Tropical oceanic cloudiness and the incidence of precipitation: Early results from CloudSat, *Geophys. Res. Lett.*, *34*, L09811, doi:10.1029/2007GL029335.

Haynes, J. M., T. S. L'Ecuyer, G. L. Stephens, S. D. Miller, C. Mitrescu, N. B. Wood, and S. Tanelli (2009), Rainfall retrieval over the ocean with spaceborne W-band radar, *J. Geophys. Res.*, doi:10.1029/2008JD009973, in press.

Held, I. M., and B. J. Soden (2000), Water vapor feedback and global warming, *Annu. Rev. Energy Environ.*, *25*, 441–475, doi:10.1146/annurev.energy.25.1.441.

Im, E. S., L. Durden, and C. Wu (2005), Cloud profiling radar for the CloudSat mission, *IEEE Trans. Aerosp. Electron. Syst.*, *20*, 15–18, doi:10.1109/RADAR.2005.1435874.

Lott, J. N., and R. Baldwin (2002), The FCC integrated surface hourly database, a new resource of global climate data, paper presented at the 13th Symposium on Global Change and Climate Variations, Am. Meteorol. Soc.Orlando, Fla., 13–17 Jan.

Petty, G.W. (1995), Frequencies and characteristics of global oceanic precipitation from shipboard present-weather reports, *Bull. Am. Meteorol. Soc.*, *76*, 1593–1616, doi:10.1175/1520-0477(1995)076<1593:FACOGO>2.0.CO;2.

Petty, G. W. (1997), An intercomparison of oceanic precipitation frequencies from 10 special sensor microwave/imager rain rate algorithms and shipboard present weather reports, *J. Geophys. Res.*, *102*, 1757–1777.

Schumacher, C., and R. A. Houze Jr. (2000), Comparison of radar data from the TRMM satellite and Kwajalein oceanic validation site, *J. Appl. Meteorol.*, *39*, 2151–2164, doi:10.1175/1520-0450(2001)040<2151:CORDFT>2.0.CO;2.

Stephens, G. L., and T. D. Ellis (2008), Controls of global-mean precipitation increases in global warming GCM experiments, *J. Clim.*, *21*, 6141–6155.

Stephens, G. L., et al. (2002), The CloudSat mission and the A-train, *Bull. Am. Meteorol. Soc.*, *83*, 1771–1790, doi:10.1175/BAMS-83-12-1771.

Stevens, B., et al. (2003), Dynamics and chemistry of marine stratocumulus–DYCOMS-II, *Bull. Am. Meteorol. Soc.*, *84*, 579–593, doi:10.1175/BAMS-84-5-579.

Sun, Y., S. Solomon, A. Dai, and R. W. Portmann (2006), How often does it rain?, *J. Clim.*, *19*, 916–934, doi:10.1175/JCLI3672.1.

Trenberth, K. E., A. Dai, R. M. Rasmussen, and D. B. Parsons (2003), The changing character of precipitation, *Bull. Am. Meteorol. Soc.*, *84*, 1205–1217, doi:10.1175/BAMS-84-9-1205.

Worley, S. J., S. D. Woodruff, R. W. Reynolds, S. J. Lubker, and N. Lott (2005), ICOADS release 2.1 data and products, *Int. J. Climatol.*, *25*, 823–842, doi:10.1002/joc.1166.

T. D. Ellis, Department of Earth Sciences, State University of New York College at Oneonta, 108 Ravine Parkway, Oneonta, NY 13820, USA. (ellistd@oneonta.edu)

J. M. Haynes, T. L'Ecuyer, and G. L. Stephens, Department of Atmospheric Science, Colorado State University, 1371 Campus Delivery, Fort Collins, CO 80523, USA. (haynes@atmos.colostate.edu; tristan@atmos.colostate.edu; stephens@atmos.colostate.edu)